Localization of a Stable Neural Correlate of Associative Memory

ARTICLE *in* SCIENCE · SEPTEMBER 2007

Impact Factor: 33.61 · DOI: 10.1126/science.1143839 · Source: PubMed

4 AUTHORS, INCLUDING:

Brian Lee Perkins
Swansea University
5 PUBLICATIONS **201** CITATIONS
SEE PROFILE

Naoki Matsuo
Osaka University
16 PUBLICATIONS **1,012** CITATIONS
SEE PROFILE

Mark Mayford
The Scripps Research Institute
57 PUBLICATIONS **6,822** CITATIONS
SEE PROFILE

Localization of a Stable Neural Correlate of Associative Memory

Leon G. Reijmers *et al.*

Science **317**, 1230 (2007);
DOI: 10.1126/science.1143839

Science (print ISSN 0036-8075; online ISSN 1095-9203) is published weekly, except the last week in December, by the American Association for the Advancement of Science, 1200 New York Avenue NW, Washington, DC 20005.

24. We thank U. Storb for the Vκ167/PEPS transgene and RSA transgenic mice; P. Glazer for Msh2$^{-/-}$ mice; S. Fugmann, M. Shlomchik, and M. Diaz for critical reading of the manuscript; G. Tokmoulina for help with cell sorting; the Yale Transgenic Mouse Service for generating transgenic mice; the Keck Facility at Yale Medical School and the Broad Institute for DNA sequencing; and the members of the Schatz lab for stimulating discussions. S.U. is a postdoctoral associate, and D.G.S. is an investigator of the Howard Hughes Medical Institute.

Supporting Online Material
www.sciencemag.org/cgi/content/full/317/5842/1227/DC1
Materials and Methods
Figs. S1 to S5
Tables S1 and S2
References

14 May 2007; accepted 18 July 2007
10.1126/science.1145065

Localization of a Stable Neural Correlate of Associative Memory

Leon G. Reijmers, Brian L. Perkins, Naoki Matsuo, Mark Mayford*

Do learning and retrieval of a memory activate the same neurons? Does the number of reactivated neurons correlate with memory strength? We developed a transgenic mouse that enables the long-lasting genetic tagging of c-*fos*–active neurons. We found neurons in the basolateral amygdala that are activated during Pavlovian fear conditioning and are reactivated during memory retrieval. The number of reactivated neurons correlated positively with the behavioral expression of the fear memory, indicating a stable neural correlate of associative memory. The ability to manipulate these neurons genetically should allow a more precise dissection of the molecular mechanisms of memory encoding within a distributed neuronal network.

Memories are presumably stored in subgroups of neurons that are activated in response to a given conjunction of sensory inputs. Sparse encoding of memories in complex neuronal networks has been identified with electrophysiological recordings of large groups of single units (*1*–*4*). Similar approaches have identified neurons with firing properties temporally linked to various aspects of task performance (*5*), and imaging techniques have enabled the physical localization of neurons that are activated during either learning or retrieval of a memory (*6*–*9*). In an associative task, the sensory stimuli and their temporal relationships differ during the learning and retrieval trial, and it is unclear to what extent the neuronal representations of these two events overlap.

We generated a transgenic mouse (TetTag mouse) that allows the persistent tagging of neurons that are activated during a given time window (Fig. 1A). The tag can be used for the direct comparison of neuronal ensemble activity at two widely spaced time points. The TetTag mouse combines elements of the tetracycline-transactivator (tTA) system for transgene regulation with neuronal activity–induced activation of the c-fos promoter to tag activated neurons (*10*–*13*). We used seizure-induced neuronal activation to test various aspects of regulation in the TetTag mouse. As shown in Fig. 1B, tau-LacZ (LAC) expression had a low baseline, could be induced broadly in the brain by seizure in a doxycycline (Dox)–regulated manner (figs. S1 and S2), and could be maintained for at least 5 days in the presence of Dox after the initial activation.

The TetTag mouse was used to determine whether neurons that are activated during learning are reactivated during retrieval. We used expression of LAC as an indicator of neuronal activity during learning and expression of the immediate-early gene *Zif/Egr* (ZIF) as an indicator of neuronal activity during retrieval (Fig. 2A) (*6*, *7*, *9*). We assessed associative memory using fear conditioning, with a focus on the learning and retrieval of a context-shock association (*14*, *15*). The basolateral amygdala (BLA) has been implicated as a potential storage site for context-shock associations (*16*–*18*). Using the

Department of Cell Biology, The Scripps Research Institute, La Jolla, CA 92037, USA.

*To whom correspondence should be addressed. E-mail: mmayford@scripps.edu

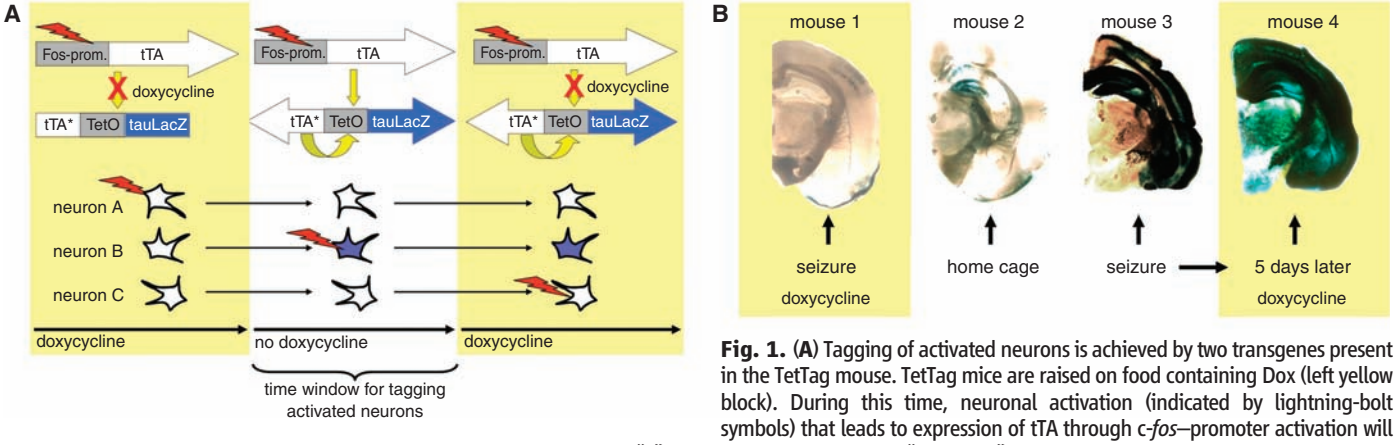

Fig. 1. (**A**) Tagging of activated neurons is achieved by two transgenes present in the TetTag mouse. TetTag mice are raised on food containing Dox (left yellow block). During this time, neuronal activation (indicated by lightning-bolt symbols) that leads to expression of tTA through c-*fos*–promoter activation will not trigger tagging, because Dox blocks activation (indicated by the red "x") of the tetO promoter (see "neuron A"). The time window for tagging is opened by switching mice to food without Dox (middle white block). Neuronal activation will now activate the transcriptional feedback loop and start expression of tau-LacZ (see "neuron B"). The time window is closed by putting mice back on Dox food (right yellow block) to block further feedback loop activation (see "neuron C"). However, neurons that were activated during the "no Dox" time window will continue to express tau-LacZ (see neuron B), because the feedback loop can maintain its own activation through the Dox-insensitive tTA^{H100Y} (tTA*), where H100Y represents His^{100}→Tyr^{100}. (**B**) Kainic acid–induced seizures were used to test whether Dox can be used to open a time window for tagging activated neurons. In the presence of Dox, no neurons are tagged after induction of seizure, as indicated by X-Gal (5-bromo-4-chloro-3-indolyl-β-D-galactopyranoside) staining of a coronal section ("mouse 1"). When a TetTag mouse is left in the home cage in the absence of Dox, only a limited number of neurons are tagged ("mouse 2"). Seizure in the absence of Dox triggers the tagging of a large number of neurons throughout the forebrain, as can be seen at 7 hours ("mouse 3") and 5 days ("mouse 4") after seizure. "Mouse 4" was put on Dox food immediately after seizure.

TetTag mice, we were able to identify neurons in the BLA that express both LAC and ZIF after learning and retrieval of conditioned fear (Fig. 2B). These reactivated neurons are probably projection neurons, because LAC neurons in the BLA did not overlap with γ-aminobutyric acid–containing neurons (fig. S3).

The experiment, outlined in Fig. 3A, used four groups of mice: The home cage (HC) group remained in the home cage throughout the experiment, the fear-conditioning (FC) group underwent fear-conditioning training and was tested for retrieval 3 days later, the fear-conditioning no-retrieval (FC-NR) group was not subjected to a retrieval test, and the no-shock (NS) group was treated identically to the FC group except that no shocks were administered. The FC group had higher freezing (lack of complete movement) scores during context retrieval than the NS group (Fig. 3B). BLA neurons activated during learning of conditioned fear were tagged, as was shown by the higher number of LAC-positive neurons in the combined FC groups as compared with those in both the HC and NS groups (Fig. 3C). This increase in LAC was not caused by retrieval-induced activation, because there was no difference between the FC and FC-NR groups [$t(16) = 0.77$]. We next asked whether neurons activated during fear conditioning were reactivated during retrieval. No significant differences in the number of ZIF neurons were found ($F_{2,29} = 0.28$); however, the FC group had a higher number of LAC+ZIF–positive neurons than the HC and NS groups (Fig. 3D). Only the FC group showed overlapping expression that was significantly higher than expected by chance (Fig. 3D). After normalizing for chance overlap, the FC group had more LAC+ZIF neurons than the HC and FC-NR groups (Fig. 3E).

Does the strength of neuronal reactivation in the BLA correlate with the strength of the memory retrieval? We used extinction to weaken the expression of the fear memory (*19*). Two groups of mice were used: The FC group was treated identically to the FC group from the previous experiment, whereas the extinction (EX) group was subjected to extinction trials between learning and retrieval (Fig. 4A). Extinc-

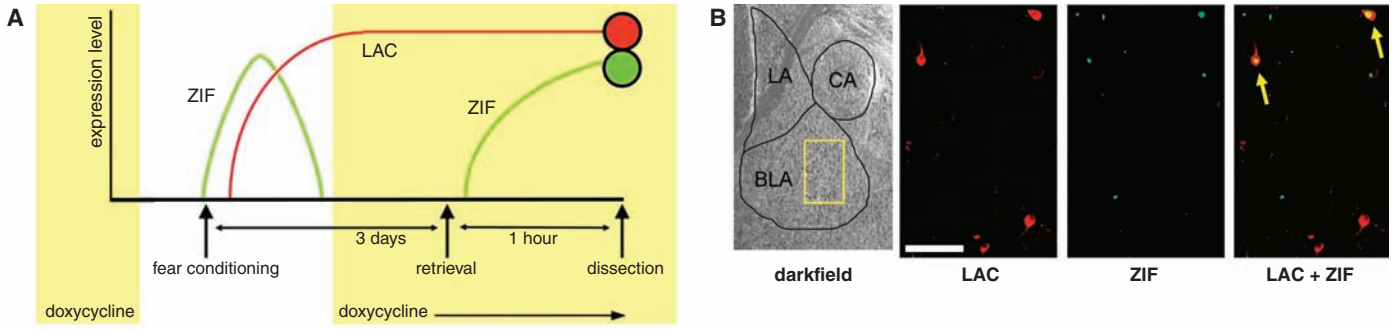

Fig. 2. (**A**) A protocol was designed to detect repeated activation of neurons during learning and retrieval of conditioned fear. Learning takes place in the absence of Dox, when activation of neurons triggers long-lasting expression of LAC and short-lasting expression of immediate-early genes like *Zif/Egr* (ZIF). Retrieval takes place 3 days after learning in the presence of Dox, which prevents activation of the molecular feedback loop. Dissection of brains is done 1 hour after retrieval, when LAC and ZIF can be used as indicators of learning-induced and retrieval-induced activation, respectively. (**B**) Example of LAC and ZIF expression in BLA neurons of a mouse that was subjected to the protocol described in (A). The yellow square in the left darkfield picture marks the area shown in the three immunostaining pictures. Yellow arrows mark neurons that express both LAC and ZIF. Scale bar, 100 μm. CA, central amygdala.

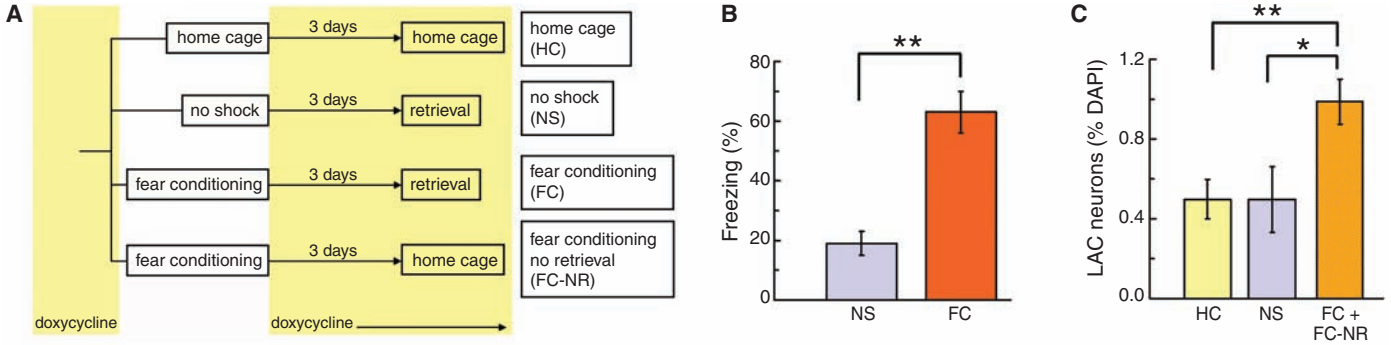

Fig. 3. Reactivated neurons in the BLA during fear conditioning provide a stable neural correlate of associative memory. (**A**) Diagram of the experimental design. HC, $n = 21$ mice; NS, $n = 10$ mice; FC, $n = 10$ mice; FC-NR, $n = 8$ mice. (**B**) The FC group showed more freezing than the NS group during context retrieval [$t(18) = 5.9$, $P = 0.00001$]. (**C**) The combined FC and FC-NR group had an increased number of LAC-positive neurons as compared with both the HC and NS groups ($F_{2,46} = 6.2$, $P = 0.004$). (**D**) The FC group had a higher number of LAC+ZIF–positive neurons than the HC and NS groups ($F_{3,45} = 7.7$, $P = 0.0003$). In the FC group, but not the other three groups, the number of LAC+ZIF neurons was higher than chance level [FC: $t(9) = 4.1$, $P = 0.003$]. (**E**) The FC group had more LAC+ZIF neurons than the HC and FC-NR groups after subtracting chance level ($F_{3,45} = 5.7$, $P = 0.002$). Data in (C) to (E) are percentages of total neurons as determined by 4′,6′-diamidino-2-phenylindole (DAPI) staining. Means ± SEM are shown in (B) to (E). *$P < 0.05$, **$P < 0.01$.

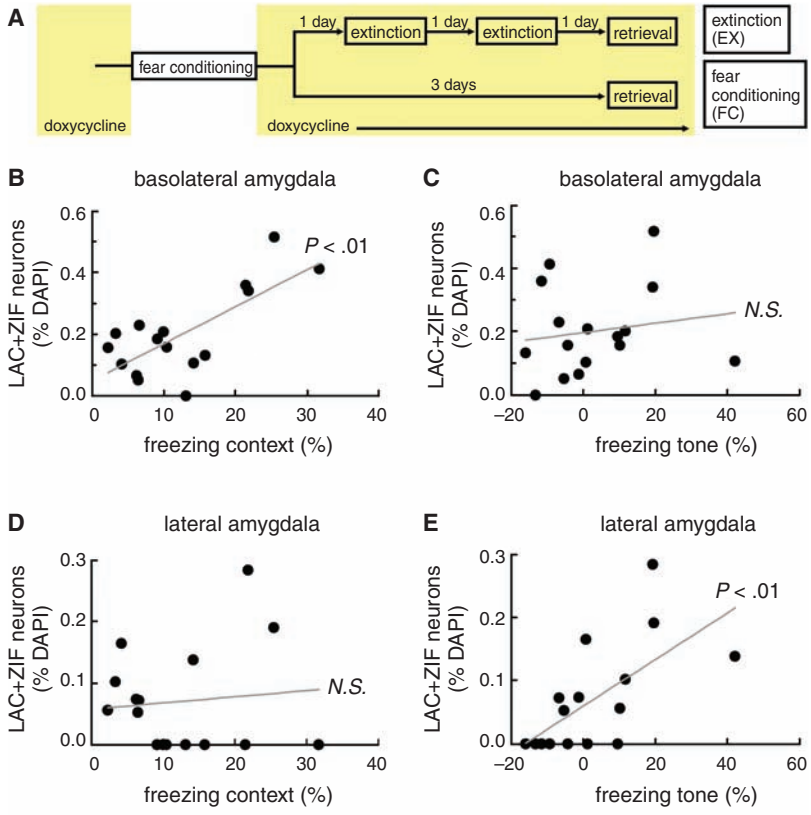

Fig. 4. The number of reactivated neurons in the BLA and LA correlates with the strength of the conditioned fear memory. (**A**) Diagram of the experimental design. EX, n = 16 mice; FC, n = 6 mice. (**B**) Within the EX group, the number of LAC+ZIF neurons in the BLA correlated with freezing during context retrieval (R = 0.73, P = 0.001). (**C**) The number of BLA LAC+ZIF neurons did not correlate with the estimated freezing during tone retrieval (R = 0.16, P = 0.6). N.S., not significant. Freezing during tone retrieval was estimated by subtracting the freezing before the first tone from the freezing during the first tone. (**D**) In the LA, the number of LAC+ZIF neurons did not correlate with freezing during context retrieval (R = 0.10, P = 0.7). (**E**) In the LA, there was a significant correlation between the number of LAC+ZIF neurons and the estimated freezing during tone retrieval (R = 0.65, P = 0.006).

tion resulted in a significant decrease in fear-memory expression, as indicated by freezing during context retrieval [EX: 13 ± 2% freezing due to context retrieval; FC: 53 ± 9%; $t(20) = 6.4$, P = 0.000003]. The EX and FC groups had similar numbers of LAC, ZIF, or LAC+ZIF neurons in the BLA ($F_{1,20} = 0.00$, $F_{1,20} = 0.34$, and $F_{1,20} = 0.61$, respectively). However, extinction showed variable effectiveness in individual mice, with freezing scores ranging from 2 to 32%. This result allowed us to look for a correlation, within a group of similarly treated mice, between the strength of (behaviorally expressed) conditioned fear and the number of reactivated neurons. Within the EX group, there was a strong correlation between the number of LAC+ZIF neurons and the freezing score measured during context retrieval (Fig. 4B). There was no correlation with LAC alone (R = 0.26, P = 0.3) or ZIF alone (R = 0.23, P = 0.4). Training, extinction, and retrieval used both the context and a tone as conditioned stimuli (CS) so that neuronal correlates of both memories could be examined. Freezing scores shown in Fig. 4B were obtained during the beginning of the retrieval test before the first tone and thus indicated contextual fear memory. We obtained an estimate of the strength of the tone fear memory by subtracting the freezing before the first tone from the freezing during the first tone. There was no correlation between the estimated freezing during tone retrieval and the number of reactivated neurons in the BLA (Fig. 4C). However, the number of reactivated neurons in the lateral amygdala (LA) correlated with the estimated freezing during tone retrieval but did not correlate with the freezing during context retrieval (Fig. 4, D and E).

We localized a group of neurons in the amygdala that was activated during learning and reactivated during retrieval of a fear memory. Reactivation of neurons in the BLA and LA correlated with contextual and tone fear memory, respectively, which is in accordance with previous studies (*17*, *18*). The reactivated neurons did not simply respond to the repeated pattern of CS (i.e., context and tone), because the unconditioned stimulus (US) (i.e., shock) was required during learning-induced activation but not during retrieval-induced reactivation. Hebbian models of plasticity postulate that synaptic weight changes should occur at synapses that are active concurrently with neuronal firing. In fear conditioning, this should occur at neurons that receive both CS and US inputs, such that the enhanced strength of the CS inputs produced by Hebbian plasticity would allow firing (or increased rates of firing) of conditioning-activated neurons in response to the CS presentation alone during the retrieval trial. This reactivation would, in effect, recapitulate aspects of the original learning episode. In the FC group, 12% of the neurons tagged with LAC were reactivated during retrieval (Fig. 3, C and D). The nonreactivated LAC cells would represent either neurons activated in the home cage (as observed in the HC group in Fig. 3C) or US-stimulated neurons that did not receive CS inputs during learning and were therefore not reactivated during retrieval. Previous studies found neurons in the BLA and LA that receive convergent projections from CS and US pathways and that can undergo fear conditioning–induced Hebbian plasticity that lasts for several hours (*4*, *16*, *20*, *21*). The current result suggests that this plasticity evolves into stable synaptic changes that confer on these neurons a capacity for reactivation by the CS that lasts for at least 3 days. The reactivated neurons seem to be a likely component of a stable engram or memory trace for conditioned fear.

The TetTag mouse provides a distinctive tool for localizing memories in a complex neuronal network. It combines the ability to image all the neurons in the region of interest with the ability to assess activation of the same neuron at widely separate time points. Because reactivation of neurons takes place in freely moving mice, it can be correlated with the behavioral expression of the memory. Use of the TetTag mouse only requires basic immunohistochemistry and microscopy tools, which are available to most researchers. The TetTag mouse not only provides a tag through the expression of a reporter gene, but can also drive the expression of additional transgenes that can be used to both follow and manipulate the physiology of the tagged neurons (*22*).

References and Notes

1. J. O'Keefe, *Exp. Neurol.* **51**, 78 (1976).
2. G. R. Sutherland, B. McNaughton, *Curr. Opin. Neurobiol.* **10**, 180 (2000).
3. R. F. Thompson, *Annu. Rev. Psychol.* **56**, 1 (2005).
4. T. Sigurdsson, V. Doyere, C. K. Cain, J. E. LeDoux, *Neuropharmacology* **52**, 215 (2007).
5. J. M. Fuster, *Neuron* **30**, 319 (2001).
6. J. Radulovic, J. Kammermeier, J. Spiess, *J. Neurosci.* **18**, 7452 (1998).
7. J. Hall, K. L. Thomas, B. J. Everitt, *J. Neurosci.* **21**, 2186 (2001).
8. W. P. Zhang, J. F. Guzowski, S. A. Thomas, *Learn. Mem.* **12**, 239 (2005).

9. J. F. Guzowski *et al.*, *Curr. Opin. Neurobiol.* **15**, 599 (2005).
10. Materials and methods are available as supporting material on *Science* Online.
11. R. J. Smeyne *et al.*, *Neuron* **8**, 13 (1992).
12. M. Gossen *et al.*, *Science* **268**, 1766 (1995).
13. M. Mayford *et al.*, *Science* **274**, 1678 (1996).
14. J. J. Kim, M. S. Fanselow, *Science* **256**, 675 (1992).
15. R. G. Phillips, J. E. LeDoux, *Behav. Neurosci.* **106**, 274 (1992).
16. S. Maren, M. S. Fanselow, *J. Neurosci.* **15**, 7548 (1995).
17. L. Calandreau, A. Desmedt, L. Decorte, R. Jaffard, *Learn. Mem.* **12**, 383 (2005).
18. L. Calandreau *et al.*, *J. Neurosci.* **26**, 13556 (2006).
19. K. M. Myers, M. Davis, *Mol. Psychiatry* **12**, 120 (2007).
20. S. Maren, *Annu. Rev. Neurosci.* **24**, 897 (2001).
21. G. J. Quirk, C. Repa, J. E. Ledoux, *Neuron* **15**, 1029 (1995).
22. F. Zhang *et al.*, *Nature* **446**, 633 (2007).
23. We thank S. G. Anagnostaras for critical reading of the manuscript and K. Spencer, T. Y. Pan, and D. Fang for excellent technical assistance. This work was supported by the NIH (National Institute of Mental Health grants 5-74653 and 57368).

Supporting Online Material
www.sciencemag.org/cgi/content/full/317/5842/1230/DC1
Materials and Methods
Figs. S1 to S3
References

16 April 2007; accepted 20 July 2007
10.1126/science.1143839

Land-Use Allocation Protects the Peruvian Amazon

Paulo J. C. Oliveira,[1] Gregory P. Asner,[1]* David E. Knapp,[1] Angélica Almeyda,[1,2] Ricardo Galván-Gildemeister,[3] Sam Keene,[4] Rebecca F. Raybin,[1] Richard C. Smith[3]

Disturbance and deforestation have profound ecological and socioeconomic effects on tropical forests, but their diffuse patterns are difficult to detect and quantify at regional scales. We expanded the Carnegie forest damage detection system to show that, between 1999 and 2005, disturbance and deforestation rates throughout the Peruvian Amazon averaged 632 square kilometers per year and 645 square kilometers per year, respectively. However, only 1 to 2% occurred within natural protected areas, indigenous territories contained only 11% of the forest disturbances and 9% of the deforestation, and recent forest concessions effectively protected against clear-cutting. Although the region shows recent increases in disturbance and deforestation rates and leakage into forests surrounding concession areas, land-use policy and remoteness are serving to protect the Peruvian Amazon.

Tropical forests play essential roles in ecological, climate, and biogeochemical processes and in the lives of human populations (*1*–*4*), but anthropogenic disturbances can disrupt forest structure, function, and composition (*5*–*7*). Because of its large, relatively contiguous area of primary rainforest, the Peruvian Amazon has major conservation value and is considered a priority in nearly all global biodiversity inventories (*8*). Despite the internationally recognized uniqueness and importance of Peruvian rainforest ecosystems, the impacts of human activities throughout the region remain poorly understood.

Increasing rates of large-scale forest damage in the neighboring Brazilian Amazon have been linked to modern road building and government policies supporting resource extraction and settlement (*9*, *10*). Peru's 661,000 km^2 of Amazon tropical forest are also subject to elevated human impacts that have not been well documented at the landscape level: The paving of the Inter-Oceanic Highway and the spreading road network throughout the Pucallpa region have brought migrants mostly from the Peruvian Andes, along with largely undocumented impacts on forest cover and structure. However, in recent years the Peruvian government has also established or extended large natural protected areas and indigenous territories in the Peruvian Amazon, and forest management legislation has placed 31% of its forests into permanent resource production status (table S9), 104,970 km^2 of which went into long-term, timber-producing, commercial concessions by 2005 (*11*). Small-scale studies have noted an increase in forest damage within some protected areas, mostly as a result of land conversion to agriculture and pasture near human settlements and river valleys (*12*) associated with proximity to roads, rural credit programs, and access to markets (*13*), as well as inadequate land-use planning and governance (*14*). However, a synoptic assessment of forest disturbance and deforestation has not been derived for Peruvian forests.

Large-scale assessments of forest disturbance in the Peruvian Amazon, typically diffuse and difficult to detect, require complex detection algorithms for the analysis of high-resolution satellite imagery (*15*, *16*), but these methods are just now proving critical for land management, conservation analysis, and land-use policy assessments in tropical forest regions (*17*). We adapted a satellite-based forest disturbance detection system, originally designed for industrial-grade timber extraction monitoring in Brazil, to Peru's generally smaller-scale forest disturbance regimes. We present an updated version of the Carnegie Landsat Analysis System (CLAS, http://asnerlab.stanford.edu) and applied it to a study area covering 79% of the Peruvian Amazon (*18*) from 1999 to 2005. The core technology of the CLAS change-detection algorithm (*15*, *19*, *20*) was improved with optimized, automated versions of the atmospheric and haze correction and the water- and/or cloud-masking processes of the Monte Carlo unmixing (AutoMCU) approach (*21*). We also added an automated deforestation-detection component to provide an integrated analysis of both diffuse forest disturbance and clear-cutting. We used 101 Landsat 5 TM (Thematic Mapper) and Landsat 7 ETM+ (Enhanced Thematic Mapper Plus) satellite images at a spatial resolution of 30 m by 30 m to derive annual incremental damage maps for most of the human-impacted, timber-producing regions—up to 24 images per year, with each nonoverlapping footprint covering 26,000 km^2. The satellite detection results were validated via a large field survey in the Pachitea and Ucayali watershed regions and regionally evaluated against available land use, land cover, and conservation maps.

We found that 632 ± 230 km^2 year^{-1} and 645 ± 325 km^2 year^{-1} of Peruvian Amazon forests were subjected to new forest disturbances and

Table 1. Forest disturbance and deforestation area estimates for Peruvian Amazon tropical forest based on CLAS methodology. The number of satellite paths per rows in each year varied according to image availability. There were 23 path/row in 1999–2000, 23 in 2000–01, and 17 in 2001–02. On the basis of an assessment of the spatial distribution of forest damage in the first 3 years, a subset of satellite path/row was selected for analyses in the following 3 years, as available: 5 path/row in 2000–03, 3 in 2003–04, and 5 in 2004–05.

Year	Damage rates (km^{-2} year^{-1})	
	Disturbed	Deforested
1999–2000	653	731
2000–2001	617	698
2001–2002	508	616
2002–2003	409	470
2003–2004	546	192
2004–2005	1070	1174
Mean	634	647

[1]Department of Global Ecology, Carnegie Institution of Washington, Stanford, CA 94305, USA. [2]Department of Anthropological Sciences, Stanford University, Stanford, CA 94305, USA. [3]Instituto del Bien Común, Avenida Petit Thouars 4377, Miraflores, Lima 18 Perú. [4]Department of Electrical and Computing Engineering, Boston University, 8 Saint Mary's Street, Boston, MA 02215, USA.

*To whom correspondence should be addressed. E-mail: gpa@stanford.edu